A Model-Based Implementation of an MPPT Technique and a Control System for a Variable Speed Wind Turbine PMSG

Najmeh Rezaei

School of Electronic Engineering and Computer Science,
Queen Mary University of London,
London E1 4NS, UK
E-mail: n.rezaei@qmul.ac.uk

Kamyar Mehran

School of Electronic Engineering and Computer Science,
Queen Mary University of London,
London E1 4NS, UK
E-mail: k.mehran@qmul.ac.uk

Calum Cossar

School of Engineering,
University of Glasgow,
Glasgow G12 8QQ, UK
E-mail: Calum.Cossar@glasgow.ac.uk.

Abstract: This paper proposes a model-based control system for a wind energy conversion system (WECS) using a direct driven permanent magnet synchronous generator (D-PMSG). The generator is connected to the grid via a back-to-back pulse-width modulation (PWM) converter with a switching frequency of 10 KHz. The integrated system model is developed in Matlab/Simulink and is based on the practical setup parameters to fully and accurately mimic the behaviour of the experimental system. A PI controller provides the generator with an optimum speed via an aerodynamic model of the wind turbine and can be readily employed for the practical setup using the designed parameters in the simulation model. A maximum power point tracking (MPPT) algorithm is further developed to ensure the maximum power captured from a wind turbine. The MPPT algorithm is simplified to reduce the computational time required for the real-time simulation.

Keywords: MPPT; PI controller; PMSG; Simulink; WECS; wind energy conversion, wind power, wind speed; wind turbine.

Biographical notes:

Najmeh Rezaei is a researcher with the School of Electronic Engineering and Computer Science at Queen Mary University of London. Her research interests include control theory in power electronics, optimisation techniques, and renewable energy systems. She is an author of a number of papers in international journals, conference proceedings, as well as a book chapter.

Kamyar Mehran is a lecturer in Power Engineering at Queen Mary University of London, UK. He completed his PhD degree at Newcastle University, UK in 2009 in Machines, Drives and Control Laboratory. Prior to his PhD, he collected over 8 years of professional experience in ICT and energy industries. His research interests include control of energy storages (grid, vehicular), high-switching power electronic converters and DC microgrids. He is active in the field of intelligent control, fuzzy systems, multi-sensory data fusion over wireless sensor networks with numerous peer-reviewed journal publications and book chapters.

Calum Cossar is a lecturer at the School of Engineering, University of Glasgow. He was a Research Assistant at the University of Glasgow in 1988 to take up a Research Assistant post in the SPEED Laboratory under the guidance of Professor Tim Miller. He was made a permanent Research Technologist in 1991 and subsequently Manager of the SPEED Lab where he was involved in over 20 industrial and government funded projects primarily investigating the control of electric motors and generators including switched reluctance and permanent magnet machines. He is co-author in over 50 publications and currently teaches Electrical Power related courses at the University of Glasgow.

1 Introduction

Wind energy is a renewable energy source that its industry is still in infancy, but due to the mandate of the Paris climate agreement in 2015, the development of wind turbine generation systems (WTGS) technology has been globally accelerated in recent years. In comparison with other renewable generation systems, WTGS have lower overall economic costs and capacity ratings and the downward trend in its costs is expected to continue (Muyee S. M., 2012; Prasad R. et al., 2009). In order to maximise the wind energy utilisation, variable speed constant frequency (VSCF) wind energy conversion systems (WECS) have been widely adopted since late 1990s (Zhu Y. et al., 2012). A rapid development of the direct-driven wind turbine (WT) with a permanent magnet synchronous generator (PMSG) in the commercial power industry has been witnessed, mainly due to its simple structure, low cost of maintenance, no gearbox requirement, high conversion efficiency, and high reliability (Polinder H. et al., 2006).

Increasing the average energy production (AEP) in wind power is mainly due to the recent developments in integrated power electronic modules. Over the last few years, the conduction/switching losses in power device modules have reduced significantly with a corresponding reduction in losses of high power converters/inverters. As a result, the full-rating inverter/converter-based wind energy conversion system using the PMSG has been widely used (Muyee S. M., 2012).

The power production capability of a wind turbine (i.e., P_{mech}), which is divided into four regions of operation, has a direct relation with the wind velocity (i.e., V) from the stationary position to the nominal and cut-out situation.

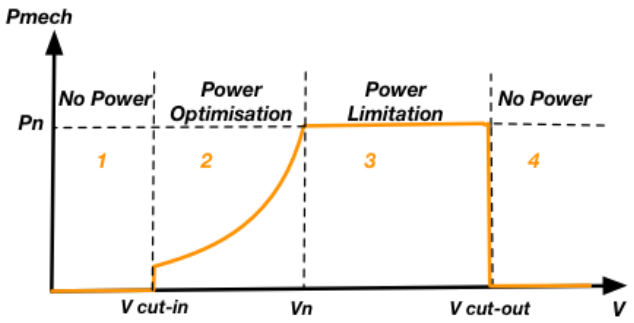

Figure 1 The ideal wind turbine power curve and its operating zones.

The region one is the startup phase, where the wind speed is too low and the torque exerted by the wind is not high enough to rotate the turbine blades. The region two is where the wind accelerates to meet "cut-in speed "which is the minimum speed for the wind turbine to rotate.The pitch angle is fixed in this region to enable the blades to receive maximum pressure from the air. As the wind speed increases, the level of output power rises rapidly until it reaches the rated value of an electrical generator and its output power. The rated wind speed (V_n) is the minimum speed that enables the wind turbine to constantly deliver its rated power. The region three is where the wind speed gets beyond the rated speed and a strong wind operating at full load. Further increase in the wind speed causes the mechanical stress on the wind turbine to reach its maximum tolerable level. Therefore, the power must be limited to protect the turbine from damaged (Zhang, X., 2013) and speed is limited to the cut-out speed. In the region four (i.e., shutting-down phase), a wind turbine is stopped from generating power (Khezami N. et al., 2012).

WECS considered in this work is called a direct drive permanent magnet synchronised generator (D-PMSG). The three-phase D-PMSG converts the mechanical power from the wind turbine into a variable voltage/frequency AC electrical power. This power is eventually converted to a DC power through a pulse width modulation (PWM) rectifier with a DC link in between in order to allow an optimal power extraction by using an MPPT algorithm. A PWM inverter ensures the injection of the produced power with a constant voltage and frequency to the power grid. The main advantages of this structure are the full decoupling between two inverters, and for the grid disturbance, the grid side converter is controlled to support the voltage recovery by supplying reactive power, while it secures the transient grid stability (Hasnaoui O. B. K. et al., 2008).

Several control techniques are suggested in the literature for the the maximum power point tracking (MPPT) technique, including the optimum tip speed ratio (TSR), hill-climbing search (HCS), and power signal feed-back (PSF), as well as the artificial intelligence (AI)-based methods, such as the fuzzy logic- and neural network-centric techniques (Thongam J. S. and Ouhrouche M., 2011). In this work, the optimum TSR is implemented to fit in the intended practical setup measurement, and to produce the maximum power tracking. The TSR control would maximise the power produced by the wind when the wind speed is below its rated value, along with limiting the electrical power by controlling the blades when the wind speed goes beyond its rated value (Azar A.T. and Serrano F.E., 2015).

Controlling the stator current, the rotor speed and the DC link voltage are the main parameters to be controlled in the PMGS wind turbine system in this work. In order to control the mentioned parameters, several PI controllers have been employed. The proportional integral derivative (PID) control is the most common control algorithm used in industry due to its functional simplicity and robust performance in a wide range of operating conditions (Priyadarshini D. and Rai S., 2014).

There have been numerous articles outlining the optimisation of energy production in wind turbines at an overall system level (Wang Q. and Chang L., 2004; Boukhezzar B. and Siguerdidjane H., 2009; Tamaarat A. and Benakcha A., 2014). In order to further these

studies, this work primarily focuses on the inner control loops of the generator using the real machine parameters and in-house laboratory optimised control algorithms to explore the actual generator performance for a variable wind regime. The main contributions can be summarised as:

- Developing a model for capturing the maximum mechanical power generated by a wind turbine using an MPPT algorithm and several PI controllers for controlling mainly the stator currents and rotor speed to have the constant DC-link voltage and to operate in the optimum range of wind speed.
- Tuning the PI controller by an experimental test at the laboratory with the in-house practical setup.

The rest of the paper is organised as follows: in Sections 2.1 and 2.2, a review of system modelling and wind turbine aerodynamics are presented, respectively. Section 2.3 describes the MPPT algorithm that has been used to maximise the power captured from the wind stream. In Section 2.4, an overall description of the PI controller used in this work is presented. In Sections 2.5 and 2.6, the machine side converter (MSC) and grid side converter (GSC) control systems are explained and their Simulink block diagrams have been presented. In Section 3, the simulation results are depicted and discussed. Finally, the conclusion is given in Section 4.

2 SYSTEM DESCRIPTION AND MODELIING

2.1 Block diagram of the system

The structure of a direct-driven PMSG wind turbine system is shown in Fig. 2. The control scheme of PMSG is a complete back-to-back converter between the PMSG and power grid with an intermediate storage capacitor. This converter connects the stator winding of the synchronous generator to the grid. The Machine-side converter (MSC) controls the active and reactive power output of the PMSG while the Grid-side converter (GSC) maintains the dc-link voltage constant and controlling the exchanged reactive power between the DC link and the grid, i.e., the active power extracted from the wind turbine is transferring to the grid at an adjustable power factor by the GSC. The dc chopper circuit, which consists of power electronic modules connected in series with the dump resistors, is used to maintain a stable dc-link voltage during power grid faults (Wu Z. et al., 2013). The main task of the PMSM control system is to control the electromagnetic torque indirectly by the sinusoidal 3-phase stator currents required to be synchronised with the respective motor phase back electromotive force (EMF). In this work, the sinusoidal pulse width modulation (SPWM) as described in (Liu Y. et al., 2016) has been used for controlling the current.

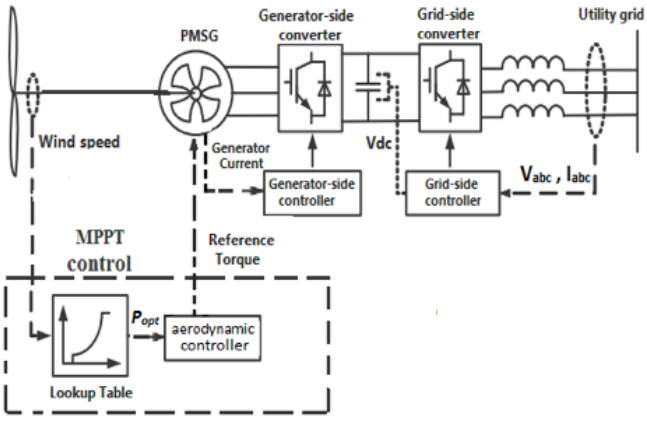

Figure 2 Block diagram of the D-PMSG wind turbine system.

2.2 Wind Turbine Aerodynamics Modelling

In the wind energy system, mechanical energy is captured in the airflow and converted to the electrical energy. Wind turbine controllers are very important for both machine operation and power production. They include sensors, controllers, power amplifiers, switches, actuators and computers/microprocessors (Manwell J.F. et al., 2010). A wind turbine must generate electricity at different wind speeds; therefore multiple control systems need to be implemented. To control the output power of the wind turbine, there are several ways depending on the design of the wind turbine and its parameters. Torque control is chosen for this study as one of the standard control methods. The wind turbine structure for the model is shown in Fig. 3.

The applied wind speed to the blades of the turbines (V) results in rotating the blades and transferring mechanical power to the shaft (P_m). The power generated in the form of kinetic energy of the air flow depends on the size of the wind turbine and wind speed. This mechanical power can be described by:

$$P_m = 0.5\,\rho\,\pi R^2\,C_P(\lambda,\beta)V^3. \tag{1}$$

where ρ is the air density (1.225 kg/m^3), R is the blade radius (m), V is the wind speed (m/s), and C_P is the

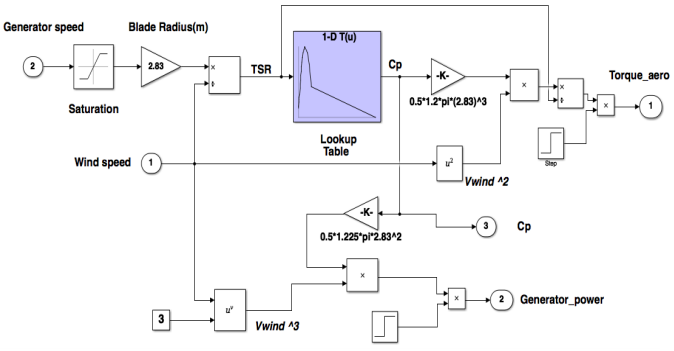

Figure 3 The wind turbine structure.

power efficiency coefficient. C_P is a non-linear power function of tip speed ratio (i.e., λ) and blade pitch angle (i.e., β), as follows:

$$\lambda = \frac{R\,\omega_t}{V}. \tag{2}$$

In Eq. 2, ω_t is the rotor angular speed of the wind turbine and R is the rotor blade radius. β is the angle between the wind flow direction and the turbine blade, which indicates how the wind velocity impacts the wind turbine blades. When $\beta = 0$, the blade is fully impacted by the wind velocity, and the wind turbine will capture the maximum power from the wind. It can be shown that the theoretical static upper limit of C_P is 16/27 (approximately 0.593). This means we can theoretically extract circa 59.3% of the kinetic energy of the wind, which is called Betz's limit (Ackermann T. ed., 2005). The power efficiency coefficient C_P, is expressed as follows (Heier S., 2014):

$$\begin{aligned} C_P(\lambda,\beta) &= C_1(C_2(\tfrac{1}{\lambda+0.08\beta} - \tfrac{0.035}{\beta^3+1}) - C_3\beta \\ &-C_4)e^{-C_5(\frac{1}{\lambda+0.08\beta} - \frac{0.035}{\beta^3+1})} + C_6\lambda. \end{aligned} \tag{3}$$

where $C_1 = 0.5109, C_2 = 116, C_3 = 0.4, C_5 = 21, C_6 = 0.0068$.

In the wind turbine structure, there are three adjustable blades of length R that are fixed on a drive shaft rotating at a speed of rotation Ω_t, connected to a gain multiplier. This multiplier rotates the electric generator. Therefore, all the three blades can be modelled as a single mechanical system which is characterised by the sum of all the mechanical characteristics. In the aerodynamic design of the blades, the coefficient of friction of the blades is very small compared to that of the air and can be neglected. Similarly, the friction losses are negligible due to the very low turbine speed (Ghoudelbourk S. et al., 2016).

Assuming a constant V, the tip speed ratio, λ, will vary proportionally to the rotational speed of the wind turbine rotor. If the $C_P(\lambda,\beta)$ curve is known for a specific fixed pitch angle of a wind turbine with a turbine rotor radius of R, it is easy to construct the curve of C_P against rotational speed for any V. Therefore, the optimal operational point of the wind turbine at a given V is determined by tracking the rotor speed to the point λ_{opt} (Ackermann T. ed., 2005).

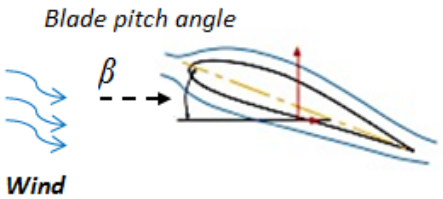

Figure 4 Representation of the blade pitch angle.

$$\lambda_{opt} = \frac{R\,\omega_t}{V}. \tag{4}$$

$$\omega_{t_{opt}} = \frac{\lambda_{opt}\,V}{R}. \tag{5}$$

For every value of V, there is an optimum rotor speed $\omega_{t_{opt}}$ which produces the maximum power recovered from the wind turbine. The aerodynamic mechanical torque on the rotating shaft (Nm) unit can then be calculated as:

$$\Gamma_m = \frac{P_m}{\omega_t}. \tag{6}$$

$$\Gamma_m = \frac{0.5\,\rho\,\pi\,R^2\,C_P\,(\lambda,\beta)\,V^3}{\omega_t}. \tag{7}$$

It is essential to maintain $\omega_t = \omega_{t_{opt}}$ to maximise P_m, which is an objective of the maximum power point tracking (MPPT) control. This means C_P has to reach its maximum value $C_{p_{\max}}$ for the maximum power to be extracted from the wind.This is implemented by controlling the electrical rotational speed of the generator rotor ω_e, which has the following relationship with ω_t as:

$$\omega_e = N_{pp}\,\omega_m. \tag{8}$$

where N_{pp} is the number of pole pairs in the PMSG, and ω_m is the mechanical rotational speed of the generator rotor (Ackermann T. ed., 2005). This mechanical speed (ω_m) accelerates or decelerates with respect to the wind turbine driving the following torque equation (Yazdani A. and Iravani R., 2010):

$$\Gamma_e - \Gamma_m = J_{eq}\frac{d\omega_m}{dt}. \tag{9}$$

where Γ_e and Γ_m are the electrical and the mechanical torque of the generator, respectively, and J_{eq} is the total equivalent inertia of the generator (the turbine inertia plus the generator inertia).

2.3 Maximum power point tracking (MPPT) control

The amount of power extracted from a WECS mainly depends on the accuracy with which the peak power points are tracked by the MPPT controller regardless of the type of generator used. In order to implement the MPPT algorithm in this system, the TSR control method has been used.

As stated before, C_P is characterised based on the different values of λ and β. For a fixed pitch angle (i.e., $\beta = 0$), a maximum C_P is obtained when the TSR is at the optimal value (λ_{opt}). For a fixed-speed wind turbine, the TSR remains constant and is independent of the wind speed. Thus, it would not operate at the peak efficiency across a range of wind speeds. Due to this reason, a variable-speed wind turbine has been considered in the presented system to operate at the

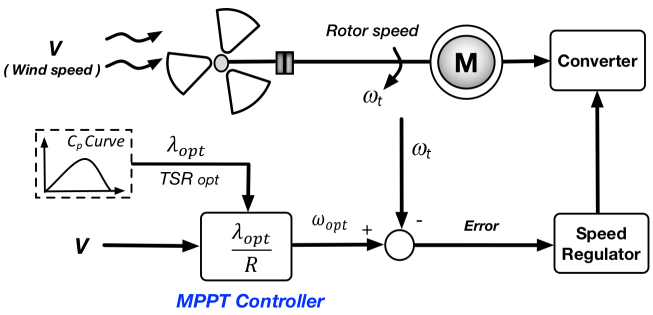

Figure 5 Block diagram of the TSR control of WECS.

maximum efficiency over all the wind speeds, and to provide the ability to control the rotor speed in favour of the presence of the power electronic converter stage between the turbine and grid. This allows the WT to operate constantly near to its optimum TSR.

The TSR control method regulates the rotational speed of the generator by forcing this speed to track the optimum rotor speed ($\omega_{t_{opt}}$). This is to maintain the TSR at the λ_{opt} value in which the extracted power is maximum. The block diagram of the TSR control method is shown in Fig. 5. The TSR value can also be determined experimentally or theoretically, as well as to be set as the reference value (Kazmi, S.M.R. et al., 2010).

2.4 Proportional integral (PI) controller

The PI controllers have been extensively used in the renewable energy conversion systems due to their satisfactory behaviour in most of the control processes, simple structure, and simple design procedure, as well as being cost-effective. The PI controller removes the error from a signal by implementing a control effect to the past and present cumulative value of the error (Lichtman A. and Fuchs P., 2017).

The digital PWM scheme that has been considered to be implemented in the current control block, is normally used with the PI controllers to improve their satisfactory dynamic response, maintain a constant switching frequency and lower acoustic noise. Tuning of the proportional gain (K_p) and integral gain (K_i) to obtain the desired control response is challenging, specifically during the commissioning of a control system. The tuning methods of PI controller are commonly classified into two main categories; closed-loop methods and open-loop ones. Tuning the controller during an automatic state in which the plant is operating in the closed loop is referred to closed-loop tuning techniques. In contrast to the closed-loop, when the plant operates in open loop and is in the manual state is categorised as the open-loop technique (Shahrokhi M. and Zomorrodi A., 2013). A comprehensive review of the different proposed methods to tune the gains of a PI regulator can be found in (Zigmund B. et al., 2006; Wang Y. G. and Shao H. H., 2000).

The background studies have shown that more focus has been put on employing the PI controllers in several MPPT control scenarios for the PMSG-based WECSs. However, there is a lack of studies reporting a practically-tuned PI controller structure for a simple and cost-effective implementation of the system. Moreover, although the non-linear controllers are becoming more widely used in the WECSs due to their better performance and stability behaviour over a wide range of uncertain wind speed variations; their design procedure tends to be more complicated. linear controllers have a simpler structure and are widely demanded in the industry.

In this work, the values of the proportional (K_p) and integral (K_i) gains, sampling time, and saturation limits, in the PI controller structure, are obtained based on the several experimental tests carried out at the University of Glasgow. The Simulink-based implementation has also verified the deployed gains. This presented model exhibits an intrinsic practicality for the effective deployment of the PI-based controller in D-PMSG WT systems.

2.5 Machine-side converter controller model

The machine-side converter (MSC) controller regulates the speed of the generator to work at the maximum power point, and to determine the required current. It has two subsystems; one is to regulate the generator speed and the other is to control the current by the PWM current control strategy.

In the speed controller block (i.e., Fig. 6), the actual rotor speed of the generator is compared with the reference speed (i.e., $\omega_{t_{opt}}$; optimum speed from the wind aerodynamics) to ensure the generator speed would track the optimum speed, and the maximum power is obtained. Then, by using a PI controller, the reference current for the current controller block is determined.

In the sinusoidal PWM current control strategy, the reference current (i.e., from the MSC speed regulator block) is introduced to a sine wave generator synchronised with the PMSG rotor position with a phase shift of 120° (i.e., Fig. 7), which results in producing

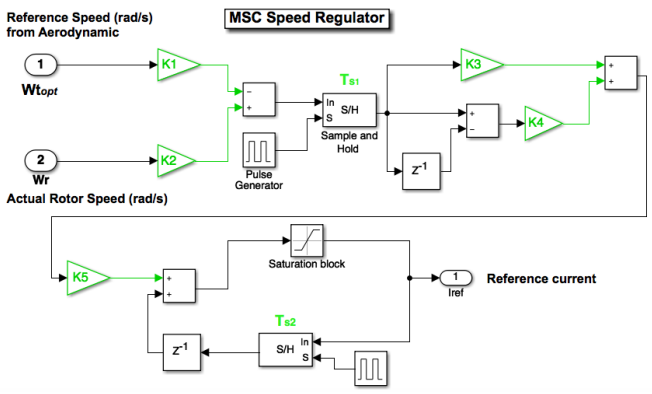

Figure 6 The MSC speed regulator.

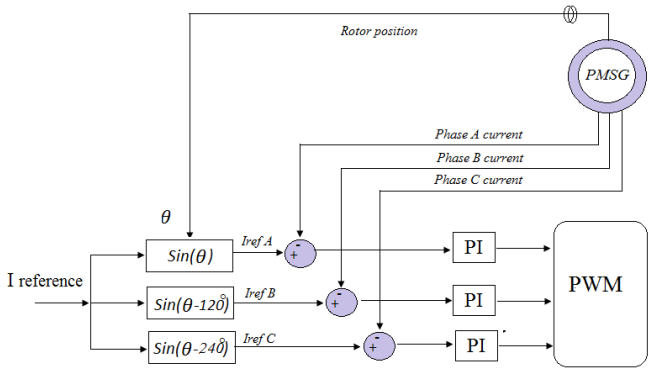

Figure 7 The sinusoidal PWM current control technique.

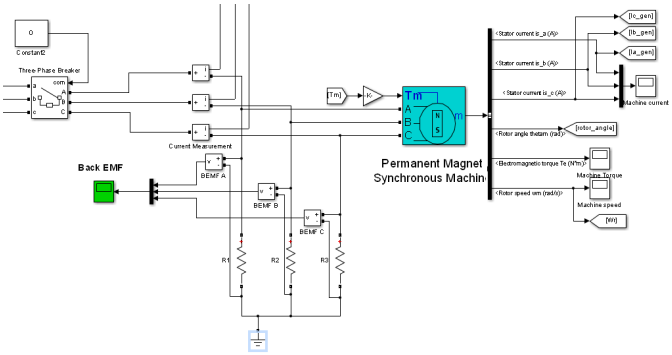

Figure 8 The generator back electromotive force (BEMF) measurement.

the sinusoidal reference current. Then, each motor phase current is compared with this current. The control block as shown in Fig. 7, includes the current control loop with three independent PI controllers for each phase current.

In practice, the generator phase back EMF to which the sinusoidal phase reference waveforms are synchronised ,should be determined. In order to investigate the required mentioned phase relationship between the generator back EMF, and the switch commutation control signals, a star connected resistor network with the inverter disconnected from the generator is carried out, as shown in Fig. 8.

In the current controller block shown in Fig. 9, the rotor position works as an input for the sine wave function blocks, which are synchronised with BEMF, to generate the proper current references, and is subsequently decoded to create the commutation signals for the upper- and lower-phase gate drivers in the MSC. This is implemented by a sine-triangle pulse width modulation (STPWM) controller. The output signal of the PI controller is compared with a $10KHz$ triangular signal to generate the control signals for the converter switches. In the PWM system, the sinusoidal control waveform sets the desired fundamental frequency of the inverter output, while the triangular waveform sets the switching frequency of the inverter.

The PI current controller for each phase is designed in z-domain to implement a discrete digital controller. As it can be seen in Fig. 11, a z-transfer function is derived by using Eq. 10. In Table 1, all the values of PI parameters for the MSC speed regulator (i.e., Fig. 6), GSC voltage regulator (i.e., Fig. 12), and z-domain current controller transfer function (i.e., Fig. 11) are listed.

$$(k_1 \times \left[u(z) \times k_2 - u(z) \times z^{-1} \times k_3\right] \times k_4) \\ +y(z) \times z^{-1} = y(z).$$

$$H(z) = \frac{y(z)}{u(z)} = k_1 \times \frac{(k_4 \times k_2 \times z) - (k_3 \times k_4)}{(z-1)}. \quad (10)$$

$$H(z) = k_1 \times k_4 \times k_2 \frac{(z - \frac{k_3}{k_2})}{(z-1)}.$$

Table 1 Parameters of the PI Controller.

Speed		Voltage		Current	
Var.	Value	Var.	Value	Var.	Value
$k_{1,2}$	128	$k_{1,2}$	128	k_1	100
k_3	21/256	k_3	21/256	k_2	21
k_4	18/128	k_4	18/128	k_3	17
k_5	1/5	k_5	1/16	k_4	1/10
$T_{s1,s2}$	$3e^{-3}$ s	$T_{s1,s2}$	$3e^{-3}$ s	T_s	$100e^{-6}$ s

2.6 Grid-side converter controller model

The grid-side converter (GSC) controller is designed to maintain a constant DC voltage in the DC bus, and to provide the required power. It is composed of two controllers for both the current and voltage. In the grid-side current regulator, in contrast to the MSC in which the generator phase current defines the phase of the reference current, the grid phase voltage determines the phase of the reference currents (i.e., the PM machine is generating).

In order to maintain the system stability, there must be a DC link voltage controller to control the amplitude of the current injected into the grid. The DC link controller regulates the relevant voltage to a given reference level (i.e., Fig. 12).

3 SIMULATION RESULTS AND DISCUSSION

A simulation model of a PMSG-based WECS is developed in this section in order to validate the presented control scheme in a practical setup. A classical method of tuning the parameters of the PI regulator, specifically, an empirical tuning method is used. All the block system parameters are listed in Table 2 (Rezaei N. et al., 2017).

The PMSG-based wind turbine is connected to the utility grid via a two-level PWM back-to-back converter. Since the DC output voltage from the converter would contain harmonics due to the switching, a series RL filter is used to filter harmonics in the voltage signals. In order

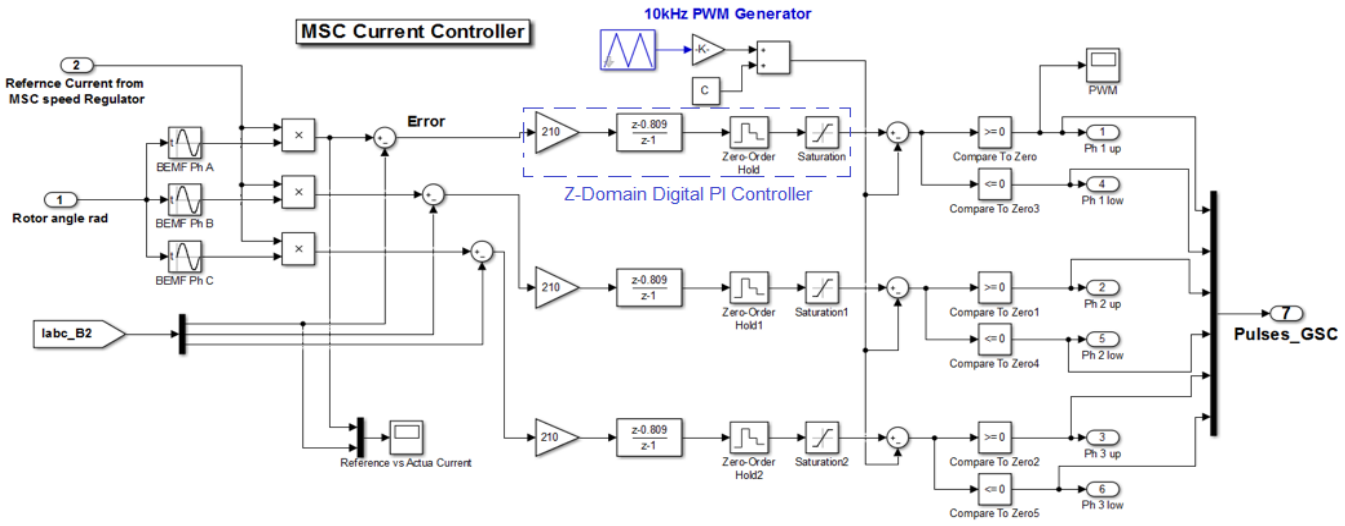

Figure 9 The MSC current controller.

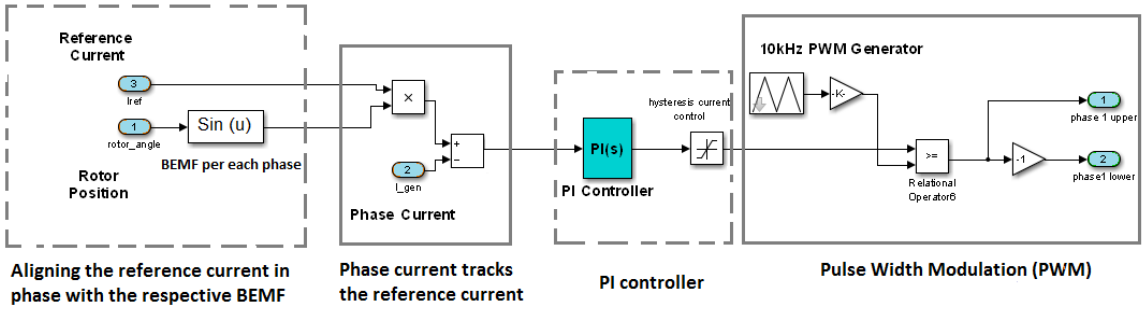

Figure 10 The current controller structure.

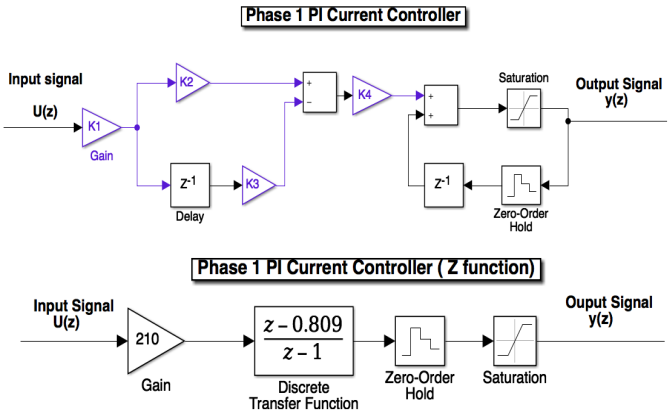

Figure 11 The z-domain PI controller transform.

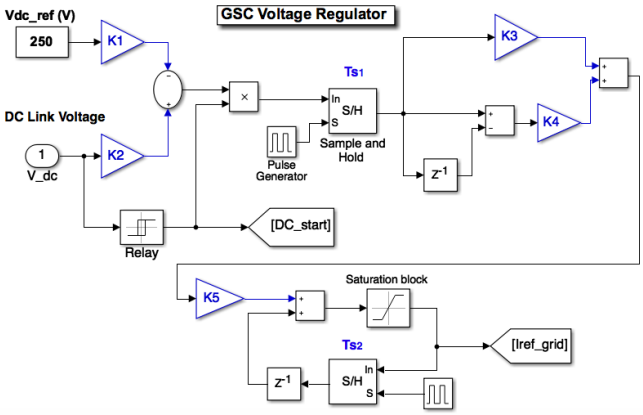

Figure 12 The grid-side converter (GSC) voltage regulator.

to acquire the generator optimum speed, the MPPT algorithm at variable wind speeds is implemented; i.e. the cut-in wind speed of 6 m/s changing gradually to the rated wind speed of 12 m/s.

The MSC and GSC modules have been developed with the two-level six IGBT switches in parallel with diodes to allow the bidirectional current flow, as well as the unidirectional voltage blocking capability. The wind speed profile is presented in Figure 14.

The main component of the Simulink model of the wind profile is a variable block which represents the changing wind speed of 6 $m/s \sim 12$ m/s. The rate limiter ensures the wind speed is not under the cut-in speed, and is not above the cut-out speed of the turbine.

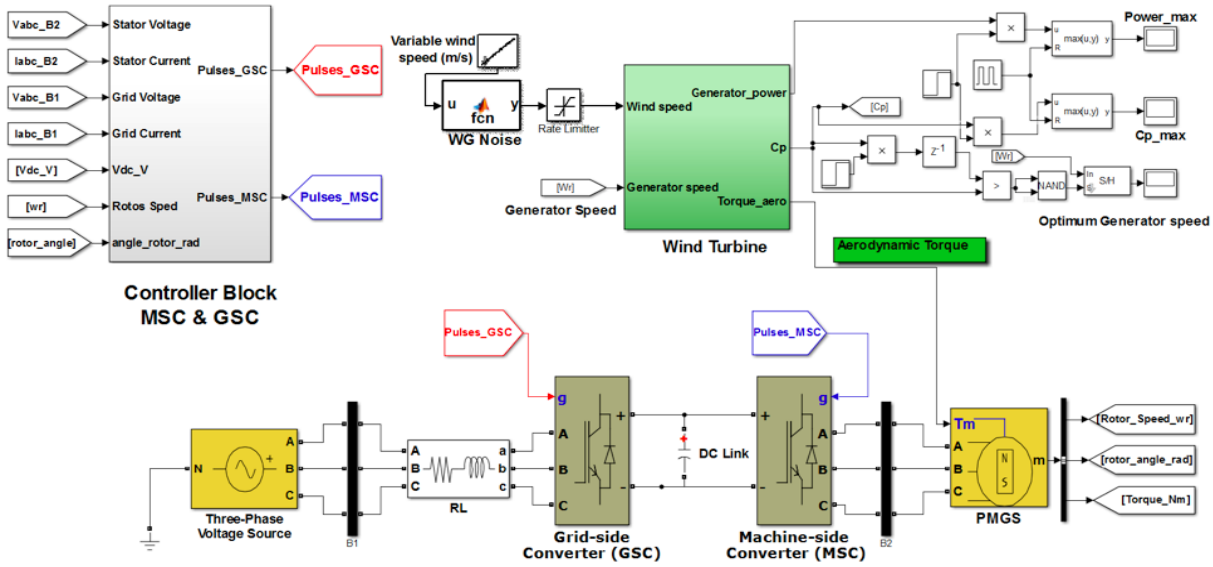

Figure 13 Permanent magnet synchronous generator based variable speed wind turbine system in MATLAB/Simulink.

Table 2 PMSG WT Drive Parameters.

Parameter	Value
WT blade radius (r)	2.83 m
WT pitch angle (β)	0 °
Maximum WT power coefficient (C_p)	0.3643
Wind speed range (V)	6 to 12 m/s
Optimum tip speed ratio (λ)	12.3
Stator resistance (R_S)	0.007 Ω
Stator inductances (L_d,L_q)	0.02 H
Magnetic flux linkage (ψ_r)	0.3 Wb
Number of poles (N_{pp})	2
Moment of inertia(J)	0.1 $kg.m^2$
PMSG's Initial speed (ω_m)	20 rad/s
PM rated power (P_m)	1.5 KW
Rotor type	Salient pole
Converter's switches (S)	IGBT-Diod
DC bus capacitor (C)	0.01 F
DC link voltage (V_{dc})	250 V
Switching frequency (f_{sw})	10 KHz
Voltage of grid (V_{rms} ph-ph) (V_{abc})	138 V
Frequency of grid (f)	50 Hz
Resistance in RL filter (R)	0.1 Ω
Inductance in RL filter (L)	10e-3 H

In order to appropriately simulate the effect of the wind speed, and to provide a more realistic representation of the mechanical output of the wind turbine, the wind speed is modelled based on the realistic scenarios. Hence, the white Gaussian noise has been added to the wind speed profile.

As shown in Fig. 15, from the beginning of the simulation until 0.1s when the reference current in machine-side (i.e., step of 0.1 s) starts to regulate the current, there is no current in the generator. In Fig. 16, the actual generator current tracks the reference current after a few milliseconds of the simulation running time. From 0.1 s to the time that the DC link capacitor is

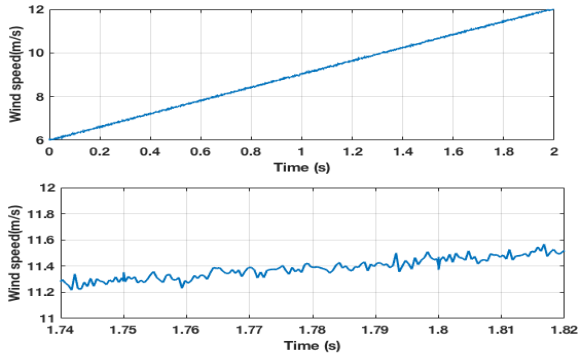

Figure 14 The wind speed profile (m/s) and its zoom plot (m/s).

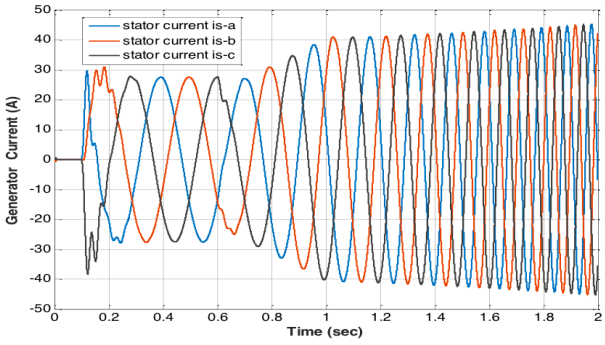

Figure 15 The generator current (A).

charged and reaches 250 V, which is 1.08 s, there is no current in the grid side, as seen in Fig. 17. The capacitor is then discharged, and the grid-side inverter is able to transfer the power. It is also evident from the grid current (i.e., Fig. 17) that the stability is early achieved to ensure the stable and efficient operation of the WECS.

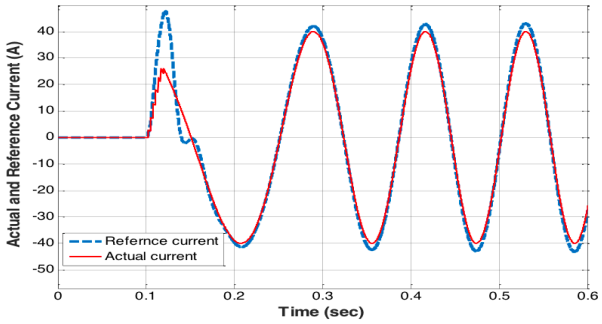

Figure 16 The actual current vs the reference current (A).

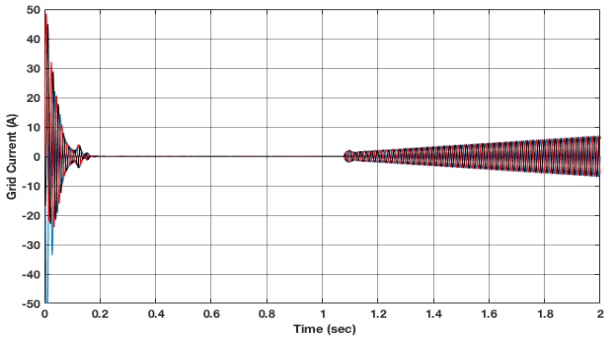

(a)

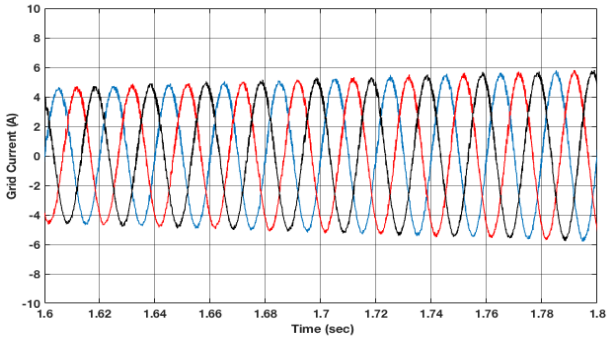

(b)

Figure 17 (a) The grid current (A), (b) The zoom plot of the grid current (A).

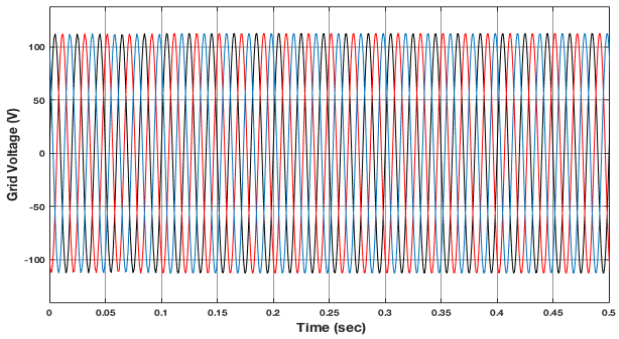

Figure 18 The grid voltage (V).

The DC link capacitor is charged by the machine-side inverter. The grid voltage is three-phase sinusoidal with the amplitude of 138 V_{rms} AC source, as seen in Fig. 18. Fig. 15 presents that the AC current in the generator is maintained below a certain range, due to the saturated input of the current controller, i.e., 50 A in this work. The generator currents; phase a, phase b and phase c; are all sinusoidal currents, and the harmonic content is observed to be minimised. Moreover, the amplitude of the current is changing since the inverter controller varies the amplitude of the current output, in order to control the DC bus voltage constant. In Fig. 19, the DC link voltage is clamped to its desirable value of 250 V, due to the activation of the threshold level in the voltage controller circuit in the grid-side controller. As a result, the DC link voltage is remained constant and stabilised at its reference value. The electromagnetic torque of the generator is also depicted in Fig. 20. The generator speed increased from its initial speed value (i.e., 20 rad/s) after 0.6 s to track the reference speed. The real power obtained from the WECS reaches its maximum available power, which is analytically calculated based on the MPPT algorithm at the variable wind speeds from 6 m/s to 12 m/s (i.e., Fig. 21).

The integrated controller can be improved by adding a pitch angle controller. When the available wind power is beyond the equipment rating, the blade pitch angle controller increases the pitch angle, in order to limit

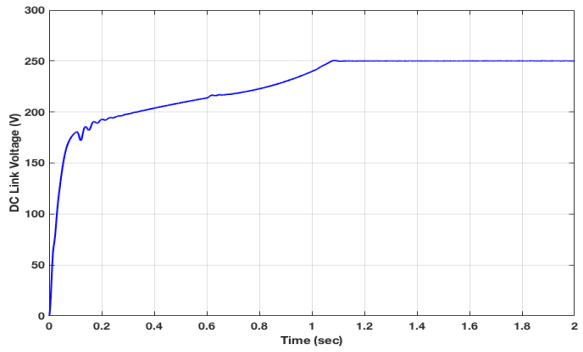

Figure 19 The DC link voltage (V).

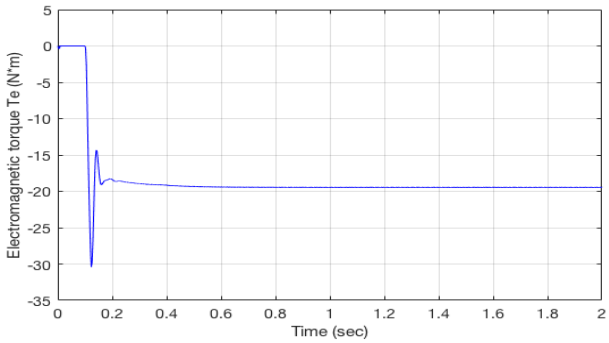

Figure 20 The electromagnetic torque (Nm) of the generator at the fixed wind speed of 10 (m/s).

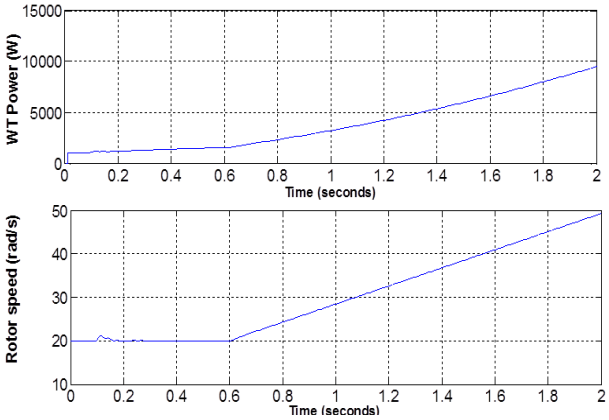

Figure 21 The generator speed (rad/s) and WT power (W) for the variable wind speed.

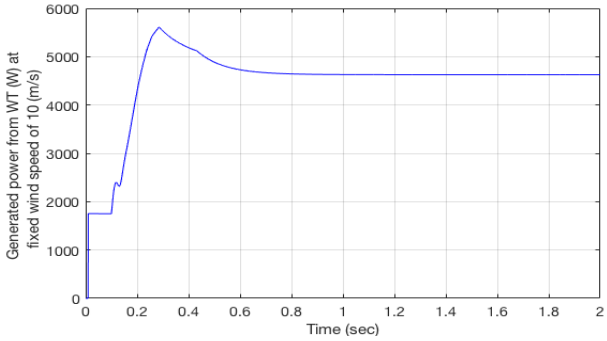

Figure 22 The power (W) captured from WT at the fixed wind speed of 10 (m/s).

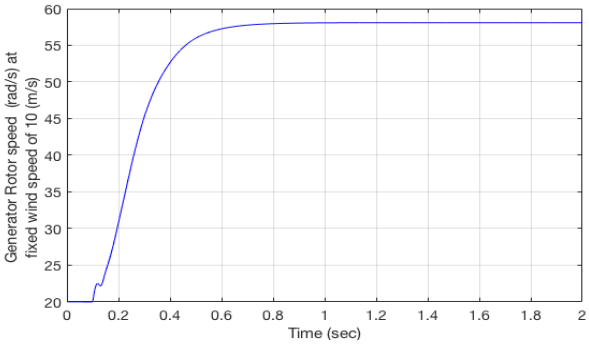

Figure 23 The generator speed (rad/s) for the fixed wind speed of 10 (m/s).

the mechanical power delivered to the shaft when the available wind power is less than the equipment rating, the blades are set at the minimum pitch to maximise the mechanical power. Various parameters in the system are chosen to provide desirable results during the entire operating range of the turbine. At the beginning of the simulation, a damped oscillation can be observed in the results due to the electrical and mechanical losses. After a period of acceleration, the electrical torque of the PM machine and wind torque enter a balanced state, and the rotor speed accelerates as the wind speed is increasing. In the case of the fixed wind speed, the rotor speed is stabilised to a constant value after acceleration, as shown in Fig. 23 for the fixed wind speed of 10 m/s.

Furthermore, systematic and mechanical limitations of the system should always be considered. For instance, in the aerodynamic section, i.e., section 2.2, to calculate the tip speed ratio (TSR), as well as the optimal TSR must be known and given to the controller; both the wind speed and turbine speed need to be also measured. The first challenge to implement the TSR control is to measure the wind speed that leads to a difficulty in practical implementation, along with the extra cost to the system. The second limitation is related to obtaining the optimal value of the TSR which is not unique, and is also dependent on the system; hence, it is different from one system to another. This mainly depends on the turbine/generator characteristics resulting in the custom-designed control software tailored for individual wind turbines (Raju A.B. et al., 2004).

4 CONCLUSION

It is shown that our presented practical control strategy is capable of actively controlling the power injected into the electric grid. The MPPT algorithm is capable of extracting maximum power from the air stream at different given wind speeds. The controller of the mechanical speed is used to ensure that the rotor speed adapts to the wind speed. This results in obtaining the optimum specific speed providing the optimum mechanical power despite the variations of the wind. The stator currents are perfectly tracking their given reference values by using the tuned PI controller in the current regulator system. The analysis of the variable speed wind turbine with direct drive permanent magnet synchronous machine shows that the developed model is suitable for small wind energy conversion systems and the validation of the practical results.

References

Ackermann, T. ed. (2005) 'Wind power in power systems', *John Wiley and Sons*.

Azar, A.T. and Serrano, F.E. (2015) 'Complex System Modelling and Control through Intelligent Soft Computations, Studies, Fuzziness and Soft Computing', *Design and modelling of anti wind up PID controllers, Springer*,Vol. 319, pp. 1–44.

Boukhezzar, B. and Siguerdidjane, H. (2009) 'Nonlinear control with wind estimation of a DFIG variable speed wind turbine for power capture optimization', *Energy Conversion and Management*,Vol. 50, No. 4, pp. 885–892.

Ghoudelbourk, S., Dib, D., Omeiri, A. and Azar, A.T. (2016) 'MPPT control in wind energy conversion

systems and the application of fractional control (PIα) in pitch wind turbine', *International Journal of Modelling, Identification and Control*,Vol. 26, No. 2, pp. 140–151.

Hasnaoui, O. B. K., Belhadj, J., and Elleuch, M. (2008) 'Direct Drive Permanent Magnet Synchronous Generator Wind Turbine investigation - Low Voltage Ride Through capability Dynamic behavior in presence of grid disturbance', *JES*, Vol. 4, No. 5, pp. 23.

Heier, S. (2014) 'Wind energy conversion systems', *Grid Integration of Wind Energy: Onshore and Offshore Conversion Systems*, pp. 31-117.

Kazmi, S.M.R., Goto, H., Guo, H.J. and Ichinokura, O. (2010) 'Review and critical analysis of the research papers published till date on maximum power point tracking in wind energy conversion system', In *Energy Conversion Congress and Exposition (ECCE)*, IEEE, pp. 4075–4082.

Khezami, N., Guillaud, X. and Benhadj, B.N. (2012) 'Multimodel LQ controller design for variable-speed and variable pitch wind turbines at high wind speeds', *International Journal of Modelling, Identification and Control*, Vol. 15, No. 2, pp.117–124.

Lichtman, A. and Fuchs, P. (2017) 'Theory of PI controller and introduction to implementation for DC motor controls', *IEEE conf. on Communication and Information Technologies (KIT)*.

Liu, Y., Abu-Rub, H., Ge, B. and Ellabban, O., (2016) 'Modulation Methods and Comparison', *Impedance source power electronic converters*, John Wiley and Sons, 2016, p. 424.

Manwell, J.F., McGowan, J.G. and Rogers, A.L. (2010) 'Wind energy explained: theory, design and application', *John Wiley and Sons*.

Muyee, S. M. (2012) 'Wind Energy Conversion Systems: Technology and Trends', *Springer-Verlag London*.

PID Theory, http://www.ni.com/white-paper/3782/en/

Polinder, H., Van der Pijl, F.F., De Vilder, G.J. and Tavner, P.J. (2006) 'Comparison of direct-drive and geared generator concepts for wind turbinesg', *IEEE Trans. on energy conversion*,Vol. 21, No. 3, pp. 725–733.

Prasad, R. Bansal, R. and Sauturaga, M. (2009) 'Wind characteristics and power density analysis for Vadra site in Fiji Islands', *International Journal of Modelling, Identification and Control (IJMIC)*,Vol. 6, No. 3, pp. 173–180.

Priyadarshini, D. and Rai, S. (2014) 'Design, Modelling and Simulation of a PID Controller for Buck Boost and Cuk Converter', *International Journal of Science and Research (IJSR)*,Vol. 3, No. 5.

Raju, A.B., Fernandes, B.G. and Chatterjee, K. (2004) 'A UPF power conditioner with maximum power point tracker for grid connected variable speed wind energy conversion system', *Power Electronics Systems and Applications. Proceedings, First International Conference on. IEEE*, pp. 107–112.

Rezaei, N., Mehran, K. and Cossar, C. 'A Practical Model and an Optimal Controller for Variable Speed Wind Turbine Permanent Magnet Synchronous Generator', *9th International Conference on Modelling, Identification and Control (ICMIC 2017)*, Kunming, 2017.

Shahrokhi, M. and Zomorrodi, A. (2013) 'Comparison of PID controller tuning methods', *Department of Chemical and Petroleum Engineering Sharif University of Technology*.

Tamaarat, A. and Benakcha, A. (2014) 'Performance of PI controller for control of active and reactive power in DFIG operating in a grid-connected variable speed wind energy conversion system', *Frontiers in Energy*,Vol. 8, No. 3, pp. 371–378.

Thongam, J. S. and Ouhrouche, M. (2011) 'MPPT control methods in wind energy conversion systems', *INTECH Open Access*.

Wang, Q. and Chang, L. (2004) 'An intelligent maximum power extraction algorithm for inverter based variable speed wind turbine systems', *IEEE Transaction Energy Conversion*,Vol. 19, No. 5, pp. 1242–1249.

Wu, Z., Dou, X., Chu, J. and Hu, M. (2013) 'Operation and control of a direct-driven PMSG-based wind turbine system with an auxiliary parallel grid-side converter', *Energies*,Vol. 6, No. 7, pp. 3405–3421.

Wang, Y. G. and Shao, H. H. (2000) 'Optimal tuning for PI controller', *Automatica*,Vol. 36, No. 1, pp. 147–152.

Yazdani, A. and Iravani, R. (2010) 'Voltage-sourced converters in power systems: modeling, control, and applications', *John Wiley and Sons*.

Zhang, X. (2013) 'Modeling and analysis of a novel wind turbine structure', *International Journal of Modelling, Identification and Control*,Vol. 19, No. 2, pp. 142–149.

Zhu, Y., Cheng, M., Hua, W. and Wang, W. (2012) 'A novel maximum power point tracking control for permanent magnet direct drive wind energy conversion systems', *Energies*,Vol. 5, No. 5, pp. 1398–1412.

Zigmund, B., Terlizzi, A.A., del Toro Garcia, X., Pavlanin, R. and Salvatore, L. (2006) 'Experimental evaluation of PI tuning techniques for field oriented control of permanent magnet synchronous motors', *Advances in Electrical and Electronic Engineering*,Vol. 5, No. 1-2, pp. 114.